iScience

CellPress
OPEN ACCESS

Article

Cavity structure-based active controllable thermal switch for battery thermal management

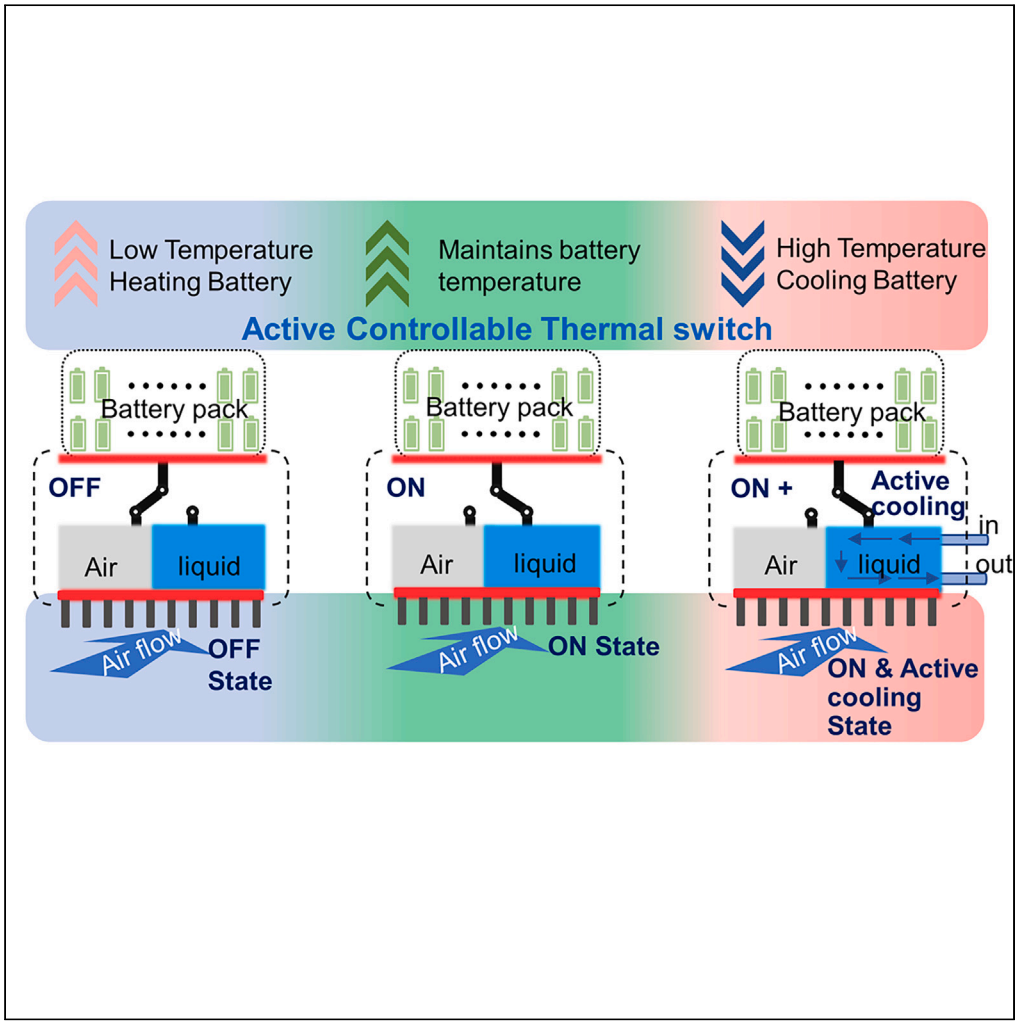

Xingzao Wang, Zhechen Guo, Jun Xu, Chenwei Shi, Xianggong Zhang, Qi Lv, Xuesong Mei

xujunx@xjtu.edu.cn

Highlights

A cavity structure based actively controllable thermal switch is proposed

The proposed thermal switch has high switch ratio with low cost

The thermal switch can be used repeatedly without performance degradation

The thermal switch has potential for real electric vehicle applications

Wang et al., iScience *26*, 108419
December 15, 2023
https://doi.org/10.1016/j.isci.2023.108419

iScience

CellPress
OPEN ACCESS

Article

Cavity structure-based active controllable thermal switch for battery thermal management

Xingzao Wang,[1,2,5] Zhechen Guo,[1,2,5] Jun Xu,[1,2,6,*] Chenwei Shi,[1,2] Xianggong Zhang,[3] Qi Lv,[4] and Xuesong Mei[1,2]

SUMMARY

Batteries may degrade fast at extreme temperatures, posing a challenge in meeting the dual requirements of heat preservation at low temperatures and efficient cooling at high temperatures. To address this issue, we propose a cavity structure-based active controllable thermal switch. It has a potential switch ratio (SR) of approximately 300, with an experimental SR of 15.4. Furthermore, the thermal resistance can be actively controlled. The "OFF State" of the thermal switch increases energy discharge at low temperatures. Pre-heating with the "OFF State" consumes only 60% of the energy required in the "ON State". By employing the "ON State" at an ambient temperature of 20°C, the battery temperature can be maintained below 35°C. And the "ON + State" keeps the maximum battery temperature remaining below 42°C under extreme conditions. These findings demonstrate that the implementation of the proposed thermal switch enhances the usability of batteries in extreme environments.

INTRODUCTION

Li-ion batteries (LIBs) serve as a prevalent power source for electric vehicles (EVs) and drones.[1–3] However, the further adoption of LIBs is hindered by their suboptimal performance at high and low temperatures.[4–6] Battery performance tends to degrade under extreme temperature conditions.[7–9] When the temperature falls below 0°C, the lithium-ion diffusivity decreases dramatically, resulting in colossal enhancement of polarization.[10–12] Therefore, the LIBs reach the cut-off voltage early in the charging and discharging cycle, and the actual capacity decreases.[13] Additionally, charging under such low temperatures can lead to severe lithium plating.[14–16] Lithium-plated batteries present safety risks of internal short circuits and thermal runaway.[17] It is also important to avoid exposing the battery to elevated temperatures. Electrolyte decomposition and solid-electrolyte interphase (SEI) growth are the primary aging mechanisms at high temperature.[18–20] The SEI layer prevents the anode from reacting with the electrolyte, and its thickening leads to a decrease in battery capacity.[21] Moreover, high temperatures due to thermal abuse can lead to potential thermal runaway.[22–24] Maintaining the temperature of LIBs within a reasonable range, regardless of environmental conditions, is crucial for energy storage systems reliant on LIBs.

The operating conditions and environment of LIBs are subject to variability. According to the specific ambient and operating conditions, the battery in a power system needs effective heat sinks to dissipate its own generated heat[25] or good insulation (in low-temperature environments) to guarantee stable operation temperature.[26,27] Use of drones in different media, such as water and air, is becoming increasingly popular.[28,29] When drones transition between these media, the ambient temperature undergoes drastic changes, negatively impacting the battery system's performance. EVs face similar challenges, particularly with the current trend toward fast charging.[30,31] The Battery Thermal Management System (BTMS) of EVs encounters conflicting demands. On the one hand, LIBs need to be heated by various methods to enhance charging and discharging performance in low-temperature conditions.[32–34] Further, batteries are usually heated before extremely fast charging to improve kinetics.[27,35,36] The BTMS should provide effective thermal insulation to prevent heat transfer to the surrounding environment. On the other hand, fast charging normally generates substantial heat that needs to be dissipated rapidly to maintain the temperature within the desired range.[37–39] However, conventional thermal devices typically exhibit a constant thermal resistance, making it challenging to adjust their thermal performance at extremely low and high temperatures.

Thermal management devices with variable thermal resistance offer a potential solution to the aforementioned conflicting challenges, as they can both retain and dissipate heat effectively.[27,40] However, their further application is hindered by limitations such as low switching ratio (SR), high costs, and complex structures. The SR refers to the ratio of thermal conductance between the ON and OFF states of the thermal switch, which is a critical performance indicator.

[1]State Key Laboratory for Manufacturing Systems Engineering, Xi'an Jiaotong University, Xi'an, Shaanxi 710049, China
[2]Shaanxi Key Laboratory of Intelligent Robots, School of Mechanical Engineering, Xi'an Jiaotong University, Xi'an, Shaanxi 710049, China
[3]Wuhan Institute of Marine Electric Propulsion, China State Shipbuilding Corporation Limited, Wuhan, Hubei 430064, China
[4]State Grid Jinhua Power Supply Company, Jinhua, Zhejiang 321000, China
[5]These author contributed equally
[6]Lead contact
*Correspondence: xujunx@xjtu.edu.cn
https://doi.org/10.1016/j.isci.2023.108419

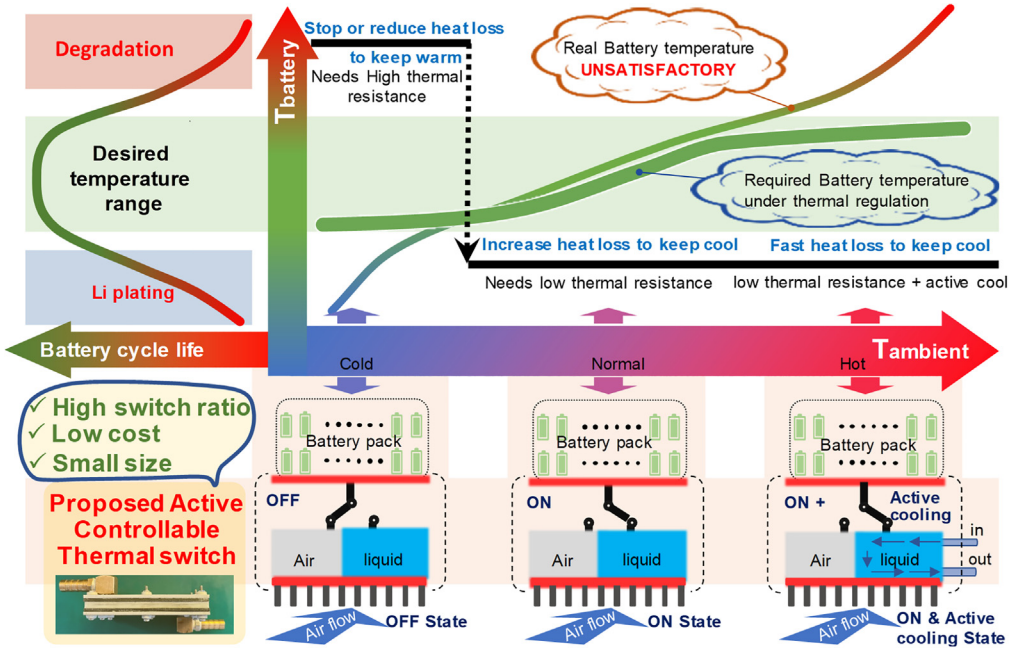

Figure 1. Batteries operating at low and high temperatures will reduce lifespan

The thermal switch regulates the battery temperature in all temperature ranges. The thermal switch has three states, "OFF State" to help warm the battery at low temperatures, "ON State" to passively cool the battery at normal temperatures, and "ON + State" to actively cool the battery at high temperatures.

Thermal switches based on phase change materials exploit the difference in thermal resistance between the two states of the material. Vanadium dioxide (VO2) exhibits a phase transition behavior from the insulating to the metallic state at about 340 K. The transition between these two states achieved an SR of 1.3:1.[41,42] In the same way: LiCoO2 (SR = 1.5:1),[43] boron nanoribbons (SR = 1.2:1).[44] Such a small SR is not suitable for battery thermal regulation. In accordance with the manner in which temperature induces phase transitions, a switch ratio of about 10 has been achieved in the study by Shrestha et al.[45] However, the phase transition temperature is 166°C. Simultaneously meeting the requirements of battery thermal regulation at both switching temperature and switching ratio is difficult for thermal switches based on material phase transitions. Further, the phase change of such materials occurs naturally based on temperature, posing challenges in realizing active control over thermal resistance.

Changes in microstructure can also lead to changes in thermal resistance. A thermal switch based on a graphene/fullerene/graphene sandwich was designed by Xue et al.[46] The thermal switch showed a switchable change in the thermal resistance of the interface by changing the amount of fullerene in the sandwich structure, resulting in an enhancement of about a factor of two in the interfacial thermal resistance during the ON/OFF State. Thermal switching based on macroscopic interfacial contact conditions provides higher SR.[40] Thermally conductive interface with or without contact depends on the different thermal expansion of different materials.[47] However, the thermal expansion of materials is typically minimal, requiring a significant total length of about 10 cm for a mere 0.1 mm variation.[47–49] HAO et al. used the heating-shortening property of shape memory alloys (SMA) to achieve contact and non-contact at the interface.[50] In this way, a lightweight design of the thermal switch was realized. However, such a structure needed movable parts that may be prone to damage, particularly in EV scenarios. Additionally, the contact surface may have some foreign objects, especially for the high dynamic applications, leading to a reduction in performance. These challenges impede the miniaturization of thermal switches and their practical implementation in real-world applications, such as EVs and drones.

To address these challenges, we propose a small-size, low-cost, active controllable thermal switch for BTMS that is applicable in both extremely hot and cold environments, as shown in Figure 1. The "OFF State" of the thermal switch is used to heat the battery at low temperature and allow the battery to fully utilize its own generated heat to maintain temperature. Meanwhile, the "ON State" of the thermal switch is designed to efficiently conduct the generated heat to avoid overheating. The proposed thermal switch demonstrates a large SR, with a potential value of approximately 300 and an experimental SR of 15.4. Furthermore, the thickness of the thermal switch is remarkably small, measuring only 10 mm, which is much smaller compared to conventional contact methods.[27,50] Additionally, the thermal switch allows for active control of thermal resistance, enabling adjustment between thermal conductivity and thermal insulation based on specific requirements. Moreover, the proposed method introduces an "ON + State" that incorporates an active cooling function to enhance the cooling capacity. In the following sections, we will present the underlying principle of this structure and validate its thermal performance. The thermal switch is applied to a BTMS in a commercial 10 Ah pouch battery, considering various ambient temperatures.

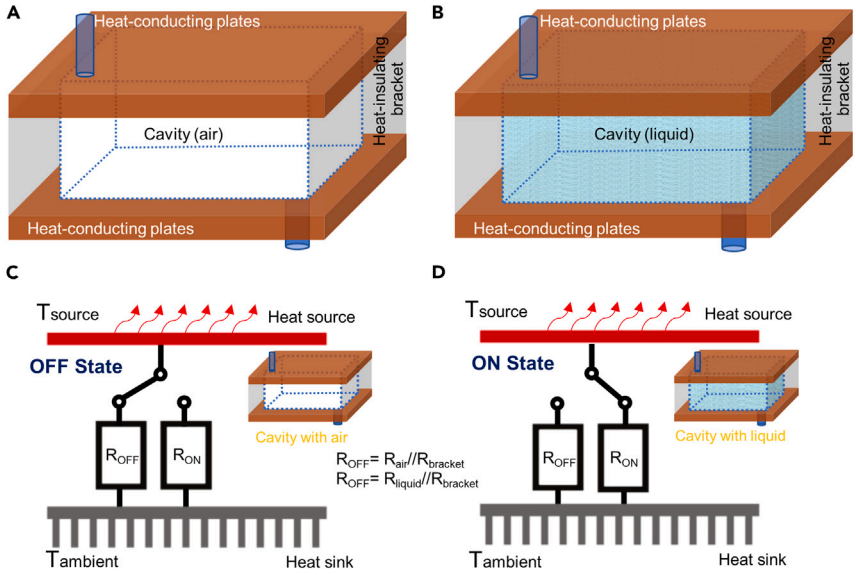

Figure 2. Design and principle of the thermal switch

(A) Design concept for the thermal switch. Two heat-conducting plates and a heat-insulating bracket form the cavity structure. When the air fills the cavity, the thermal switch is the "OFF State".

(B) When the liquid fills the cavity, the thermal switch is the "ON State".

(C)Thermal switch is thermally insulating when the cavity is filled with air, and a small amount of heat can only be conducted through the bracket.

(D) The thermal switch is thermally conductive when the cavity is filled with liquid and a large amount of heat transfers through the liquid.

RESULTS

The thermal switch concept and structure

Existing thermal switches still suffer from low SR, large-size, and high-cost problems, which can be solved by the cavity structure-based thermal switch proposed in this paper. As shown in Figures 2A and 2B, the proposed thermal switch is a cavity structure. Figure S1 shows the fabrication details of the thermal switch. The main components of this thermal switch are the upper and lower heat-conducting plates and the heat-insulating bracket. When the cavity is filled with air, the heat is mainly conducted through the bracket, and the thermal resistance is high. When the cavity is filled with liquid, the heat is mainly conducted through the liquid, resulting in low thermal resistance. Selecting the cavity as liquid or air is equivalent to turning ON/OFF the thermal switch, as shown in Figures 2C and 2D. Higher SR can be achieved using liquids with higher thermal conductivity. Liquid metal such as mercury has a thermal conductivity of 8.36 W/(m·K), meaning the theoretical SR can be up to about 300. To ensure safety, the experiment of this paper uses water as the heat-conducting fluid to verify the concept. The thermal conductivity of liquid (e.g., water), air, and heat-insulation bracket (rubber) is 0.59 W/(m·K), 0.0267 W/(m·K), and 0.20 W/(m·K), respectively. Thus, the experimental SR is 15.4.

Switch ratio, reliability, and cycling

An experimental setup is designed to verify the proposed thermal switch, as shown in Figure 3A. The lower aluminum bar contacts with a thermostatic aluminum plate on the bottom surface and with the thermal switch on the top surface. The upper aluminum bar contacts with a cooling aluminum plate on the top surface (maintaining the upper bar temperature at approximately −15°C when turned to the "OFF State"). All contact surfaces in Figure 3A are fully covered with silicone grease for thermal conductivity. The thermally insulating foam (not shown in Figure 3A) around the aluminum bar is used to minimize the influence of ambient. Thermocouples probed into the center of the aluminum bar are used to obtain the temperature gradient, as shown in Figure 3A. The heat flux q in the aluminum bar can be calculated by Fourier's law:

$$q = k\frac{dT}{dz} \qquad \text{(Equation 1)}$$

where k is the thermal conductivity of aluminum and dT/dz is the temperature gradient in the bars.

The thermal switch can change the thermal resistance as required at any temperature. The temperature of the heating and cooling plates is set constant, and the switching ratio can be calculated from the temperature gradient at a steady state. A complete cycle is shown in Figure 3B. When the "OFF State" is selected, the aluminum bars have almost no temperature gradient ($T_6 \approx T_5 \approx T_4$, $T_3 \approx T_2 \approx T_1$). It means that the thermal switch insulates the conduction of heat. When the thermal switch turns to the "ON State," the three low bar temperature monitoring points rise above 10°C, and the temperature gradient increases significantly.

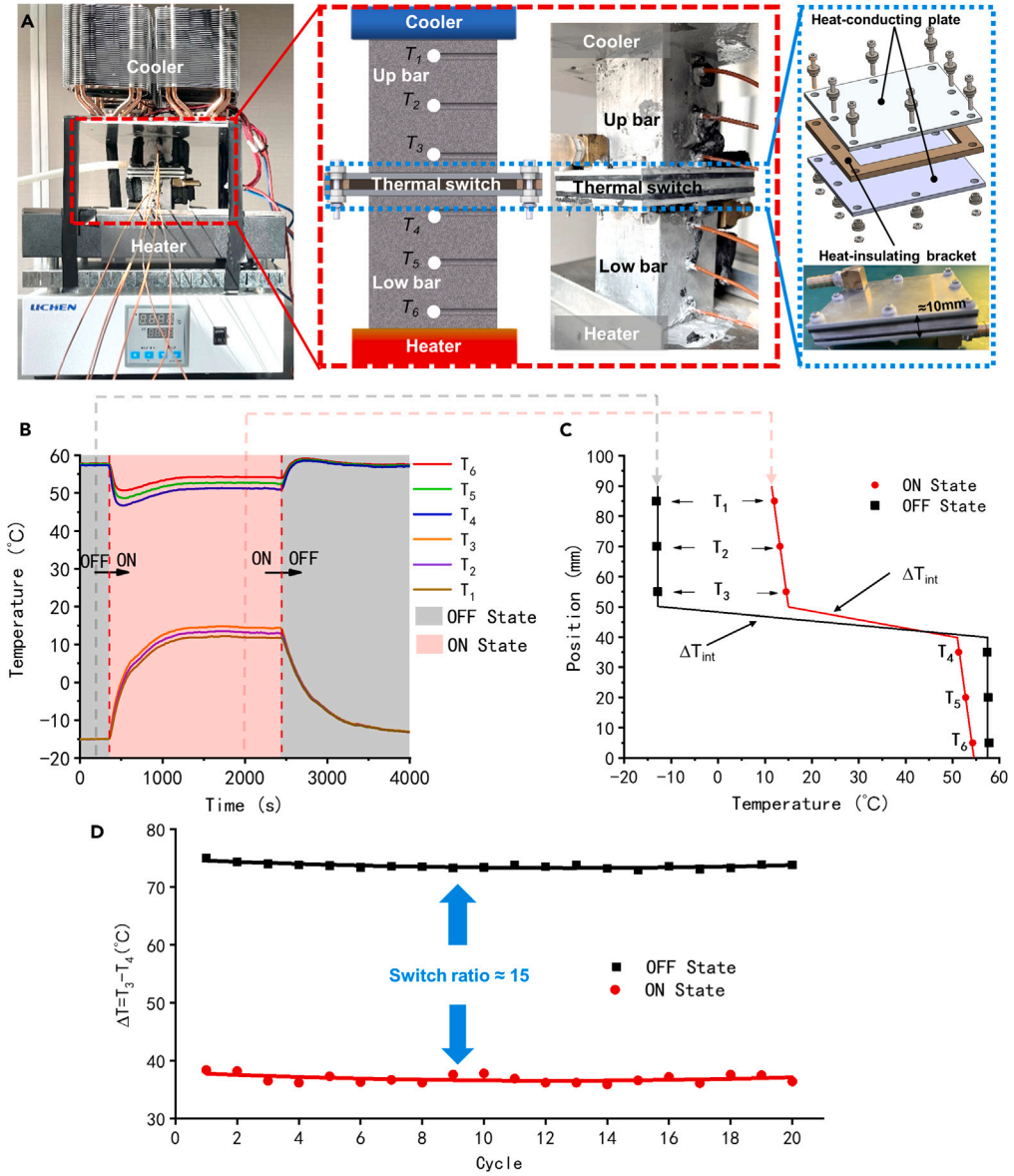

Figure 3. Validation of the proposed thermal switch

(A) Schematic of the experimental setup. Six thermocouples probing into the aluminum bar are used to obtain the temperature gradient, which is used to calculate the heat flux and temperature discontinuity ΔT_{int} at the thermal switch interface.

(B) Temperature data in the aluminum bar during the steady state in one ON/OFF cycle.

(C) Temperature gradient at steady-state ("ON State"/"OFF State"). Temperature data are taken from Figure 3B.

(D) The temperature difference T_3-T_4 remains almost constant during the 20 cycles, which can demonstrate the sustainability of the proposed thermal switch performance.

Figure 3C clearly displayed the "ON State" and the "OFF State" temperature at steady state. The temperature difference ΔT_{int} between the upper and lower interface can be obtained by linear interpolation of the temperature gradient shown in Figure 3C. S is the contact area between the aluminum bar and the thermal switch. The thermal resistance R of the thermal switch can be obtained from the following equation:

$$R = \frac{\Delta T_{int}}{q \cdot S} \quad \text{(Equation 2)}$$

As a result, $R_{on} \approx 1.12$°C/W, $R_{off} \approx 17.25$°C/W, and SR $\approx$ 15.4, as obtained from the steady-state temperature data by Equations 1 and 2.

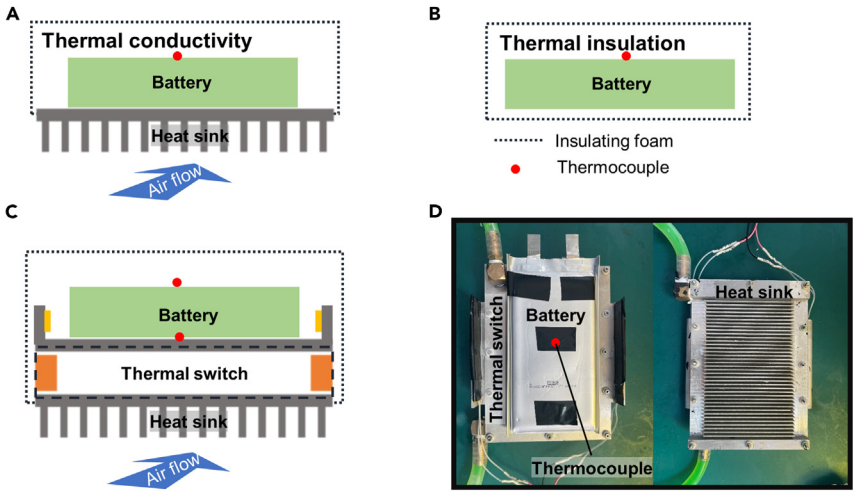

Figure 4. Application in battery thermal management system

(A) The "thermal conductivity design," the battery is covered with insulating foam except for the bottom side.

(B) The "thermal insulation design," all sides of the battery are covered with insulating foam.

(C) A commercial pouch battery is installed on the thermal switch for testing. Two thermocouples for measuring the temperature of the battery and the heat plates.

(D) Photos of test components.

To further study the reliability and life performance of the thermal switch in temperature regulation, the system is repeatedly cycled for 20 cycles, switching between the "ON State" and the "OFF State". The results of $\Delta T = T_3\text{-}T_4$ are shown in Figure 3D. The ΔT remains almost constant for each steady state ($\Delta T \approx 74°C$ for the "OFF State" and $\Delta T \approx 37°C$ for the "OFF State"). In fact, based on the principle of regulating thermal resistance, the proposed thermal switch can be used almost indefinitely without performance degradation.

Application in battery thermal management system and comparison

The battery pack is normally placed at the bottom of the vehicle chassis, and the bottom side is in contact with air. Based on this reality, there are two normal BTMS designs. The first is the "thermal conductivity design," where thermal conductivity is needed for heat dissipation. The other is the "thermal insulation design," where batteries need to be insulated at low temperatures. According to the scenario of battery layout on EVs, these two cases are designed, as shown in Figures 4A and 4B, respectively. However, these two BTMS are only applicable to partial scenarios due to material and structure limitations. In this work, the proposed thermal switch can fit various environments and operating conditions. Different states can be selected according to the actual needs of the BTMS. The proposed thermal switch structure can be appropriately arranged between the battery and the heat sink, thus resulting in a BTMS with a controllable thermal resistance function, as shown in Figure 4C.

Further, when thermal switches are applied to a battery pack, multiple distributed thermal switches can be used to improve the temperature uniformity of the batteries in the battery pack. Thermal switches can be controlled to reduce the thermal resistance in the high-temperature region and increase the thermal resistance in the low-temperature region. In order to conveniently validate the proposed method, the BTMS is fabricated for a single battery with the proposed thermal switch, as shown in Figure 4D. In order to comprehensively examine the thermal characteristics of these three structures, three common usage scenarios of EVs are designed in this paper.

Multi-environment testing and comparison

The liquid flow in the thermal switch cavity offers the additional function-active cooling, referred to as the "ON + State". Heat transfer always requires a temperature difference. A thermal switch with low thermal resistance cannot cool the battery when the ambient temperature reaches 40°C. Under more extreme application conditions, at 40°C ambient temperature with a 3C rate, for example, the proposed thermal switch can cool the battery effectively, as shown in Figure 5A. The battery's temperature with the "thermal insulation design" rises to 60°C. Battery temperature with the "thermal conductivity design" rises a little lower but also reaches 58.1°C at the end of discharge. Such high temperatures accelerate battery aging and increase the risk of thermal runaway. As a comparison, the battery temperature under active cooling of the "ON + State" of the thermal switch is maintained at a little over 40°C. The "ON + State" of the thermal switch can also be used in fast charging, which is considered as the most unfavorable EV usage scenario for cooling.

For a typical EV application scenario with an ambient temperature of 20°C, the thermal switch should be turned to the "ON State" to conduct more heat, reduce the battery temperature, and save energy. In such a scenario, the temperature difference between the battery

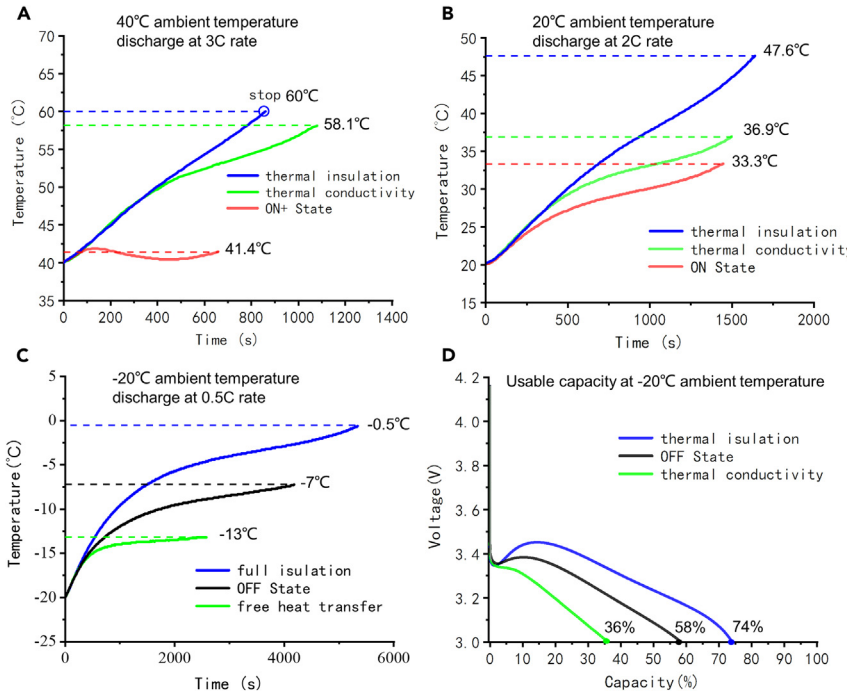

Figure 5. Application in battery thermal management system in multi-environment

(A) Temperature rising comparison in three cases (ambient temperature = 40°C). The "thermal insulation design" stop discharging when the temperature rises to 60°C.

(B) Temperature rising comparison in three cases (ambient temperature = 20°C).

(C) Temperature rising comparison in three cases (ambient temperature = −20°C).

(D) Capacity comparison in three cases (ambient temperature = −20°C) For each test, the battery is fully charged at 20°C and achieved thermal equilibrium with low-temperature environments (−20°C) before discharging at 0.5 C rate.

and the environment can be used to dissipate heat with the "ON State" of the thermal switch. The discharge rate is increased to 2 C to cover more EV application scenarios. As shown in Figure 5B, the "thermal insulation design" rises to 47.6°C at the end of discharge. The "ON State" of the thermal switch rises to 33.3°C. It has a lower temperature than the "thermal conductivity design," since the liquid has a high specific heat capacity and absorbs extra heat. At the same time, it indicates that the equivalent thermal resistance of the "ON State" of the thermal switch is smaller than the "thermal conductivity design".

At an ambient temperature of −20°C, the experiments compared the battery performance under the "OFF State" of the thermal switch, the "thermal conductivity design," and the "thermal insulation design". Due to the increase in internal resistance of the battery at low temperatures, the battery is discharged at 0.5 C to avoid reaching the cut-off voltage instantly. Figure 5C illustrates that the battery's temperature increases in all three cases. At the end of discharge, the temperature of the "thermal insulation design" rises to −0.5°C, which gets the highest temperature for its good insulation. As a comparison, the "thermal conductivity design" only rises to −13°C. The temperature of the "OFF State" of the thermal switch is between these two cases, which rises to −7°C at the end of discharge. Only about 36% discharge capacity can be used at low temperatures for the "thermal conductivity design," as shown in Figure 5D. For this reason, the "thermal insulation design" retains 74% discharge capacity, as shown in Figure 5D, which is the ideal condition for its good insulation. The "OFF State" of the thermal switch configuration retains 58% discharge capacity, also between the "thermal insulation design" and the "thermal conductivity design". During the discharge process, the voltage under the "thermal conductivity design" continued to drop. In contrast, the voltages under both the "OFF State" and the "thermal insulation design" recovered to varying degrees due to the enhanced kinetics and transport by the elevated temperature. From Figures 5C and 5D, the degree of voltage recovery is positively correlated with the temperature rise.

Low-temperature pre-heating testing

To improve low-temperature capability further, the BTMS is configured with a pre-heat function, as shown in Figures 6A and 6B. Heating plates are powered by the battery and placed on the heat-conducting plate. The heating power can be expressed as

$$Q = I^2 \cdot (R_{bat} + R_{heat}) \quad \text{(Equation 3)}$$

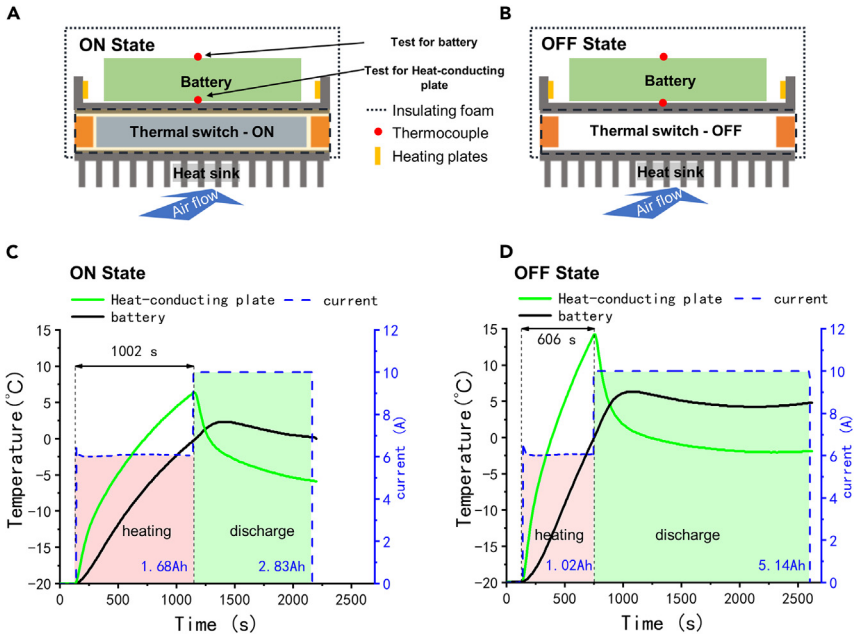

Figures 6. Battery pre-heating experiment equipped with the proposed thermal switch

(A and B) A schematic diagram of the experimental setup. The ON State: the cavity is filled with water. The OFF State: the cavity is filled with air. A commercial pouch battery is installed on the thermal switch for testing. Two thermocouples for measuring the battery and the heat-conducting plate temperature.

(C and D) Battery and heat-conducting plate temperature profile during heating and discharging. The heating process stops when the measured temperature of the battery reaches 0°C. The blue profile represents the battery discharge current. The red region represents the capacity consumption of the self-heating, while the green region represents the battery discharge capacity.

When pre-heating, the thermal switch should limit the heat transfer to the environment, which can shorten the heating time and reduce the energy consumed for heating. In order to verify this performance of the thermal switch, pre-heating experiments are carried out with both the "ON State" and the "OFF State" of the thermal switch. The heating cut-off condition is that the measurement temperature rises to 0°C to ensure the whole battery temperature is larger than 0°C. The heating current in these two cases is about 6 A, as shown in Figures 6C and 6D. As illustrated in Figures 6C and 6D, the battery temperature of the "OFF State" rises faster than the "ON State" during pre-heating. It takes 1002 s and 1.68 Ah for the "ON State" for the battery temperature to rise to 0°C. As a comparison, it needs 606 s and 1.02 Ah for the "OFF State," about 60% of the energy needed for pre-heating with the "ON State". The high thermal resistance of the "OFF State" prevents heat transfer to the environment. As a result, it heats faster and consumes less energy.

After the battery is heated, it proceeds to the discharge step. The "OFF State" of the thermal switch, characterized by high thermal resistance, effectively retains the generated heat. As shown in Figures 6C and 6D, the green region represents the "OFF State" maintaining the battery temperature at around 5°C during discharge, while the "ON State" fails to maintain the temperature. Notably, with the battery temperature being higher in the "OFF State," a discharge capacity of 5.14 Ah is achieved, which is 1.8 times higher than the discharge capacity of 2.83 Ah in the "ON State". The proposed thermal switch enables flexible control of thermal resistance, thereby enhancing heating performance regardless of the heating method employed.

DISCUSSION

In this paper, a cavity structure-based active controllable thermal switch has been proposed to solve the critical requirements for alternating hot and cold ambient applications. The proposed thermal switch exhibits a potential switch ratio (SR) of approximately 300, with an experimental SR of 15.4. Notably, the thermal switch does not contain any movable parts, making its structure simple and ensuring a virtually infinite lifespan. This thermal switch effectively cools the battery in high-temperature environments while retaining the battery's heat in low-temperature environments.

When adjusted to "ON + State," the thermal switch can effectively cool the battery at an ambient temperature of 40°C. At the same time, the good thermal conductivity of the thermal switch in the "ON state" is also able to cool the battery in a room temperature environment (20°C).

In the "OFF state," the thermal switch retains most of the heat generated by the battery to be used to increase the temperature, further enhancing kinetics and transportation. As a result, battery low-temperature discharge capacity increased by 61%. At the same heating setting, the electric power required for low-temperature heating is reduced by 60% when the thermal switch is in the "OFF state".

In summary, the proposed cavity structure-based thermal switch shows promising potential for integration with a BMS. It can be customized by adjusting the edge length to fit the actual battery pack size and can further evolve toward miniaturization for real EV applications.

Limitations of the study

This paper explores the use of thermal switches to improve the use of batteries in various extreme environments. Therefore, the performance of the thermal switch is experimentally analyzed. The effect of thermal switches on the temperature of the cell capacity of the battery is also analyzed. But how this thermal switch can further improve the performance of battery module usage needs to be further investigated in future work.

STAR★METHODS

Detailed methods are provided in the online version of this paper and include the following:

- KEY RESOURCES TABLE
- RESOURCE AVAILABILITY
  - Lead contact
  - Materials availability
  - Data and code availability
- EXPERIMENTAL MODEL AND STUDY PARTICIPANT DETAILS
- METHOD DETAILS
  - Switch ratio testing method
  - Multi-environment testing method
- QUANTIFICATION AND STATISTICAL ANALYSIS
- ADDITIONAL RESOURCES

SUPPLEMENTAL INFORMATION

Supplemental information can be found online at https://doi.org/10.1016/j.isci.2023.108419.

ACKNOWLEDGMENTS

This work was supported by the National Natural Science Foundation of China (52075420) and the National Key Research and Development Program of China (2020YFB1708400).

AUTHOR CONTRIBUTIONS

J.X., X.W., and Z.G. conceptualized the research. X.W., Z.G., C.S. X.Z., and Q.L. analyzed the battery data. X.W., Z.G., and C.S designed the experiments and validated the method. J.X., X.W., and Z. G. wrote the original draft preparation. All authors reviewed and edited the manuscript. All authors contributed to discussions of data and manuscript review.

DECLARATION OF INTERESTS

The authors declare no competing interest.

INCLUSION AND DIVERSITY

We support inclusive, diverse, and equitable conduct of research.

Received: September 18, 2023
Revised: October 30, 2023
Accepted: November 7, 2023
Published: November 9, 2023

REFERENCES

1. Zhu, J., Wang, Y., Huang, Y., Bhushan Gopaluni, R., Cao, Y., Heere, M., Mühlbauer, M.J., Mereacre, L., Dai, H., Liu, X., et al. (2022). Data-driven capacity estimation of commercial lithium-ion batteries from voltage relaxation. Nat. Commun. *13*, 2261.
2. Jones, P.K., Stimming, U., and Lee, A.A. (2022). Impedance-based forecasting of lithium-ion battery performance amid uneven usage. Nat. Commun. *13*, 4806.
3. Lin, C., Xu, J., and Mei, X. (2023). Improving state-of-health estimation for lithium-ion batteries via unlabeled charging data. Energy Storage Mater. *54*, 85–97.
4. Wang, Q., Jiang, B., Li, B., and Yan, Y. (2016). A critical review of thermal management models and solutions of lithium-ion batteries for the development of pure electric vehicles. Renew. Sustain. Energy Rev. *64*, 106–128.
5. Yuksel, T., and Michalek, J.J. (2015). Effects of regional temperature on electric vehicle efficiency, range, and emissions in the United States. Environ. Sci. Technol. *49*, 3974–3980.
6. Xu, J., Guo, Z., Wang, X., Xu, Z., and Mei, X. (2023). Battery thermal modeling and effective cooling/heating methods. In Handbook of Thermal Management Systems, F. Aloui, E.G. Varuvel, and A. Sonthalia, eds. (Elsevier), pp. 175–202.
7. Leng, F., Tan, C.M., and Pecht, M. (2015). Effect of Temperature on the Aging rate of Li Ion Battery Operating above Room Temperature. Sci. Rep. *5*, 12967.
8. Ruan, H., Barreras, J.V., Steinhardt, M., Jossen, A., Offer, G.J., and Wu, B. (2023). The heating triangle: A quantitative review of self-heating methods for lithium-ion batteries at

low temperatures. J. Power Sources *581*, 233484.
9. Xu, J., Mei, X., Wang, X., Fu, Y., Zhao, Y., and Wang, J. (2021). A Relative State of Health Estimation Method Based on Wavelet Analysis for Lithium-Ion Battery Cells. IEEE Trans. Ind. Electron. *68*, 6973–6981.
10. Jaguemont, J., Boulon, L., and Dubé, Y. (2016). A comprehensive review of lithium-ion batteries used in hybrid and electric vehicles at cold temperatures. Appl. Energy *164*, 99–114.
11. Tippmann, S., Walper, D., Balboa, L., Spier, B., and Bessler, W.G. (2014). Low-temperature charging of lithium-ion cells part I: Electrochemical modeling and experimental investigation of degradation behavior. J. Power Sources *252*, 305–316.
12. Xiong, R., Li, Z., Yang, R., Shen, W., Ma, S., and Sun, F. (2022). Fast self-heating battery with anti-aging awareness for freezing climates application. Appl. Energy *324*, 119762.
13. Liu, H., Wei, Z., He, W., and Zhao, J. (2017). Thermal issues about Li-ion batteries and recent progress in battery thermal management systems: A review. Energy Convers. Manag. *150*, 304–330.
14. Ruan, H., Jiang, J., Sun, B., Su, X., He, X., and Zhao, K. (2019). An optimal internal-heating strategy for lithium-ion batteries at low temperature considering both heating time and lifetime reduction. Appl. Energy *256*, 113797.
15. Zhang, L., Liu, L., Gao, X., Pan, Y., Liu, X., and Feng, X. (2022). Modeling of Lithium plating in lithium ion batteries based on Monte Carlo method. J. Power Sources *541*, 231568.
16. Waldmann, T., Hogg, B.-I., and Wohlfahrt-Mehrens, M. (2018). Li plating as unwanted side reaction in commercial Li-ion cells – A review. J. Power Sources *384*, 107–124.
17. Feng, X., Ouyang, M., Liu, X., Lu, L., Xia, Y., and He, X. (2018). Thermal runaway mechanism of lithium ion battery for electric vehicles: A review. Energy Storage Mater. *10*, 246–267.
18. Yang, X.-G., Liu, T., Gao, Y., Ge, S., Leng, Y., Wang, D., and Wang, C.-Y. (2019). Asymmetric Temperature Modulation for Extreme Fast Charging of Lithium-Ion Batteries. Joule *3*, 3002–3019.
19. Wang, C.Y., Liu, T., Yang, X.G., Ge, S., Stanley, N.V., Rountree, E.S., Leng, Y., and McCarthy, B.D. (2022). Fast charging of energy-dense lithium-ion batteries. Nature *611*, 485–490.
20. Liu, J., Zhang, Y., Bai, J., Zhou, L., and Wang, Z. (2023). Influence of lithium plating on lithium-ion battery aging at high temperature. Electrochim. Acta *454*, 142362.
21. Gao, T., Bai, J., Ouyang, D., Wang, Z., Bai, W., Mao, N., and Zhu, Y. (2023). Effect of aging temperature on thermal stability of lithium-ion batteries: Part A – High-temperature aging. Renew. Energy *203*, 592–600.
22. Shahid, S., and Agelin-Chaab, M. (2022). A review of thermal runaway prevention and mitigation strategies for lithium-ion batteries. Energy Convers. Manag. X *16*, 100310.
23. Xiao, Y., Yan, M., Shi, L., Gong, L., Cheng, X., Zhang, H., and Pan, Y. (2023). High-temperature resistant, super elastic aerogel sheet prepared based on in-situ supercritical separation method for thermal runaway prohibition of lithium-ion batteries. Energy Storage Mater. *61*, 102871.
24. Hasan, H.A., Togun, H., Abed, A.M., Biswas, N., and Mohammed, H.I. (2023). Thermal performance assessment for an array of cylindrical Lithium-Ion battery cells using an Air-Cooling system. Appl. Energy *346*, 121354.
25. Guo, Z., Xu, J., Wang, X., and Mei, X. (2023). Fast multilayer temperature distribution estimation for lithium-ion battery pack. eTransportation *18*, 100266.
26. Du, T., Xiong, Z., Delgado, L., Liao, W., Peoples, J., Kantharaj, R., Chowdhury, P.R., Marconnet, A., and Ruan, X. (2021). Wide range continuously tunable and fast thermal switching based on compressible graphene composite foams. Nat. Commun. *12*, 4915.
27. Zeng, Y., Zhang, B., Fu, Y., Shen, F., Zheng, Q., Chalise, D., Miao, R., Kaur, S., Lubner, S.D., Tucker, M.C., et al. (2023). Extreme fast charging of commercial Li-ion batteries via combined thermal switching and self-heating approaches. Nat. Commun. *14*, 3229.
28. Li, L., Wang, S., Zhang, Y., Song, S., Wang, C., Tan, S., Zhao, W., Wang, G., Sun, W., Yang, F., et al. (2022). Aerial-aquatic robots capable of crossing the air-water boundary and hitchhiking on surfaces. Sci. Robot. *7*, eabm6695.
29. Xu, J., Guo, Z., Xu, Z., Zhou, X., and Mei, X. (2023). A systematic review and comparison of liquid-based cooling system for lithium-ion batteries. eTransportation *17*, 100242.
30. Liu, Y., Zhu, Y., and Cui, Y. (2019). Challenges and opportunities towards fast-charging battery materials. Nat. Energy *4*, 540–550.
31. Huang, W., Ye, Y., Chen, H., Vilá, R.A., Xiang, A., Wang, H., Liu, F., Yu, Z., Xu, J., Zhang, Z., et al. (2022). Onboard early detection and mitigation of lithium plating in fast-charging batteries. Nat. Commun. *13*, 7091.
32. Xu, J., Mei, X., Wang, H., and Wang, J. (2021). A Hybrid Self-Heating Method for Batteries Used at Low Temperature. IEEE Trans. Ind. Inf. *17*, 4714–4723.
33. Wang, C.Y., Zhang, G., Ge, S., Xu, T., Ji, Y., Yang, X.G., and Leng, Y. (2016). Lithium-ion battery structure that self-heats at low temperatures. Nature *529*, 515–518.
34. Ruan, H., Jiang, J., Sun, B., Zhang, W., Gao, W., Wang, L.Y., and Ma, Z. (2016). A rapid low-temperature internal heating strategy with optimal frequency based on constant polarization voltage for lithium-ion batteries. Appl. Energy *177*, 771–782.
35. Yang, X.-G., Liu, T., and Wang, C.-Y. (2021). Thermally modulated lithium iron phosphate batteries for mass-market electric vehicles. Nat. Energy *6*, 176–185.
36. Yang, X.-G., Zhang, G., Ge, S., and Wang, C.-Y. (2018). Fast charging of lithium-ion batteries at all temperatures. Proc. Natl. Acad. Sci. USA *115*, 7266–7271.
37. Jin, X., Duan, X., Jiang, W., Wang, Y., Zou, Y., Lei, W., Sun, L., and Ma, Z. (2021). Structural design of a composite board/heat pipe based on the coupled electro-chemical-thermal model in battery thermal management system. Energy *216*, 119234.
38. Liu, Z., Zeng, X., Zhao, W., Gao, Y., Sun, Y., and Yan, P. (2022). A topology optimization design of three-dimensional cooling plate for the thermal homogeneity of lithium-ion batteries. Energy Convers. Manag. X *14*, 100215.
39. Guo, Z., Xu, J., Wang, X., Shi, J., Li, E., and Mei, X. (2023). Fine Thermal Control Based on Multilayer Temperature Distribution for Lithium-Ion Batteries. IEEE Trans. Ind. Inf. 1–12.
40. Miao, R., Kishore, R., Kaur, S., Prasher, R., and Dames, C. (2022). A non-volatile thermal switch for building energy savings. Cell Reports Physical Science *3*, 100960.
41. Zhu, J., Hippalgaonkar, K., Shen, S., Wang, K., Abate, Y., Lee, S., Wu, J., Yin, X., Majumdar, A., and Zhang, X. (2014). Temperature-gated thermal rectifier for active heat flow control. Nano Lett. *14*, 4867–4872.
42. Ito, K., Nishikawa, K., Iizuka, H., and Toshiyoshi, H. (2014). Experimental investigation of radiative thermal rectifier using vanadium dioxide. Appl. Phys. Lett. *105*.
43. Cho, J., Losego, M.D., Zhang, H.G., Kim, H., Zuo, J., Petrov, I., Cahill, D.G., and Braun, P.V. (2014). Electrochemically tunable thermal conductivity of lithium cobalt oxide. Nat. Commun. *5*, 4035.
44. Yang, J., Yang, Y., Waltermire, S.W., Wu, X., Zhang, H., Gutu, T., Jiang, Y., Chen, Y., Zinn, A.A., Prasher, R., et al. (2011). Enhanced and switchable nanoscale thermal conduction due to van der Waals interfaces. Nat. Nanotechnol. *7*, 91–95.
45. Shrestha, R., Luan, Y., Shin, S., Zhang, T., Luo, X., Lundh, J.S., Gong, W., Bockstaller, M.R., Choi, S., Luo, T., et al. (2019). High-contrast and reversible polymer thermal regulator by structural phase transition. Sci. Adv. *5*, eaax3777.
46. Xue, Y., Park, H.S., and Jiang, J.-W. (2023). On/off switchable interfacial thermal resistance in graphene/fullerene/graphene heterostructures. Int. J. Heat Mass Tran. *212*, 124222.
47. Guo, L., Zhang, X., Huang, Y., Hu, R., and Liu, C. (2017). Thermal characterization of a new differential thermal expansion heat switch for space optical remote sensor. Appl. Therm. Eng. *113*, 1242–1249.
48. Nohara, T., Shinozaki, K., Ando, M., Okamoto, A., Sugita, H., and Takada, S. (2013). Development of Mechanical Heat Switch for Future Space Mission. The Proceedings of the Thermal Engineering Conference *2013*, 119–120.
49. Marland, B., Bugby, D., and Stouffer, C. (2004). Development and testing of an advanced cryogenic thermal switch and cryogenic thermal switch test bed. Cryogenics *44*, 413–420.
50. Hao, M., Li, J., Park, S., Moura, S., and Dames, C. (2018). Efficient thermal management of Li-ion batteries with a passive interfacial thermal regulator based on a shape memory alloy. Nat. Energy *3*, 899–906.

STAR★METHODS

KEY RESOURCES TABLE

REAGENT or RESOURCE	SOURCE	IDENTIFIER
Critical commercial assays		
Battery	DFD	D12B5X4WR00BB
Battery test device	Arbin LBT21	https://arbin.com
Software and algorithms		
MATLAB 2020	Mathworks	https://www.mathworks.com/products/matlab.html

RESOURCE AVAILABILITY

Lead contact

Further information and requests for resources should be directed to and will be fulfilled by the lead contact, Jun Xu (xujunx@xjtu.edu.cn)

Materials availability

- The pouch battery used in this study can be get from (https://www.dfdchem.com/).
- This study did not generate new unique reagents.

Data and code availability

- The published article includes all [datasets/code] generated or analyzed during this study.
- This paper does not report original code.
- Any additional information required to reanalyze the data reported in this paper is available from the lead contact upon request.

EXPERIMENTAL MODEL AND STUDY PARTICIPANT DETAILS

Our study does not use experimental models typical in the life sciences.

METHOD DETAILS

Two experimental methods used in the paper are listed in the follows.

Switch ratio testing method

During the experiment, the operating conditions of the heating and cooling plates are set and then held. Keep the thermal switch at the 'OFF State' until the system reaches temperature steady state, as shown in Figure 3B. Next, the liquid is injected into the thermal switch cavity, and the thermal switch is turned to the 'ON State'. In the process, T type thermocouples of 1mm diameter are used for measuring the temperature profile, and the data are sent to the computer via serial port and recorded. Using the temperature data, the SR of the thermal switch can be calculated. In this way, the thermal switch completes a cycle of states. Aluminum bars are surrounded by insulation foam to reduce heat exchange with the environment. Silicone grease is used to reduce the thermal interface resistance between the bars and the thermal switch.

Multi-environment testing method

A 10 Ah lithium pouch battery is fully charged (1 C, 4.2 V) before each test. The battery is placed in a chamber for more than 12 h before the testing. Silicone grease is used to reduce the thermal resistance between the pouch battery and the heat-conducting plate. Three experimental temperatures are set up to cover the most practical usage scenarios.

(1) Extreme High Temperature Environment (40°C). The cooling performance of the 'ON + State' is compared with 'thermal insulation' and 'thermal conductivity' at 3C discharge and 40°C. Due to overheating (temperature >60°C), the 'thermal insulation' was stopped halfway.
(2) Ordinary temperature environment (20°C). The 'ON State' is compared with 'thermal insulation' and 'thermal conductivity' at 2 C discharge and 20°C.
(3) Low-temperature environment (−20°C). The thermal switch should be turned to 'OFF State' before the test. Then, the 'OFF State' is compared with 'thermal insulation', and 'thermal conductivity' at 0.5 C discharge and −20°C. In Figures 5A and 5B, to heat the battery faster, a 1.3 ohm resistor is installed on the heat-conducting plate and the resistor is powered by the battery.

QUANTIFICATION AND STATISTICAL ANALYSIS

Our study does not include statistical analysis or quantification.

ADDITIONAL RESOURCES

Our study has not generated or contributed to a new website/forum or if it is not part of a clinical trial.